JOURNAL OF MATERIALS SCIENCE 15 (1980) 1701–1708

Phase relations and ordering in the dysprosia-zirconia system

C. PASCUAL, P. DURAN
Instituto de Cerámica y Vidrio, Special Ceramics Division, Arganda del Rey, Madrid, Spain

The phase diagram in the subsolidus for the system Dy_2O_3–ZrO_2 has been established. The areas of existence of the high temperature solid solutions based on ZrO_2 and Dy_2O_3 were determined using the precision lattice parameter method. At low temperature, long-range ordering occured in the Dy_2O_3-rich region ($>$ 50 mol % Dy_2O_3) and two hexagonal compounds of an $M_7O_{11.5}$- and M_7O_{11}-type were found. The first of these compounds is formed at about 55 mol % Dy_2O_3 and possesses a very narrow homogeneity range. At approximately 1750° C this compound undergoes a transformation into cubic solid solutions of fluorite and C-type. The second is formed within the Dy_2O_3 concentration range between ~ 65 and 90 mol % Dy_2O_3. Above 1700° C the hexagonal compound Dy_6ZrO_{11} undergoes a transformation into a cubic solid solution of C-type.

1. Introduction

The first reported phase diagram for the zirconia–dysprosia system was that by Perez y Jorba [1]. A significant feature of his results is the existence of a miscibility gap in the type C region suggested by the co-existence of two type C phases. A complex picture of phase transformations was revealed for this system, but since it was not wholly consistent his results should be treated with care. At high temperatures, a continuous transition between flourite and C-type solid solution was also reported. This result was confirmed by Rouanet [2] who determined the liquidus and found a eutectic point at ~ 80 mol % Dy_2O_3.

In both works above the ZrO_2-rich portion was not studied with the required precision. Therefore, the purposed of this paper is to investigate the doubtful regions such as the ZrO_2-rich portion, to determine the extent of the zirconia and dysprosia solid solutions and the existence and stability of the ordered phases.

2. Experimental technique

The zirconia and dysprosia raw materials were 99.8% and 99.9% pure, respectively. Mixed oxides were prepared by grinding the components together in an agate mortar, pressed into small pellets, and fired at 1300° C for several hours before further treatment. The samples were subsequently sintered above 1800° C or melted in a solar furnace. After they were fired, the samples were reground and portions from each were again pressed and heat-treated (up to 1765° C) in air, using a superkanthal furnace up to 1550° C and a molybdenum-wound furnace with protected windings or a special gas furnace above 1550° C. A few high-temperature treatments at ~ 2000° C were conducted in a flowing Ar–5% H_2 atmoshpere, cooling the pellets as rapidly as possible (10 min from 2000° C to 500° C).

Temperature was controlled within ± 5° C by conventional electronic controllers. Up to 1750° C the pellets were enclosed in Pt-foil and bound with Pt-wire to the hot junction of the Pt–6% Rh/Pt–30% Rh thermocouple used. Above 1750° C, the temperature was measured with an optical pyrometer calibrated at the melting point of alumina, and the precision of the temperature measurements was no better than ± 20° C. The samples were held at the required temperature for long enough to establish equilibrium and then air-quenched by rapid withdrawal from the furnace and allowed to cool to room temperature before being examined by X-ray diffraction. The heating times were 3h

0022–2461/80/071701–08$02.80/0

at 2000° C, 10 h at 1765° C, 385 h at 1450° C and 2 to 6 months at 800° to 1150° C.

The phases present in the quenched samples were identified by X-ray diffraction and the phase boundaries of the cubic field were determined from precision lattice parameter measurements. The scan rate was $\frac{1}{4}^\circ$ 2θ min^{-1} in the direction of increasing 2θ. Only high-angle peaks ($2\theta > 60^\circ$) were used to calculate precise lattice parameters, A lattice parameter was calculated from each line and these data were plotted as a function of $\frac{1}{2}$ ($\cos 2\theta/\sin\theta + \cos^2\theta/\theta$) to obtain the corrected value of the lattice parameter a_0. The experimental limits of each lattice parameter were determined by the deviation of the experimental points from the calculated least squares curve.

High-temperature X-ray diffraction analyses were conducted in air (room temperature to 1500° C) on specimens containing from 0 to 10 mol % Dy_2O_3. The heating element was made of ductile Pt-40 Rh. A thin film of vaseline was applied to the heater and a few milligrams of ground material were deposited. The specimen-coated heater was then aligned in a diffractometer and the wax burned off. For phase identification, only the low 2θ angles containing (111) and (200) peaks were scanned. Temperatures were measured to ± 2° C with a Pt–6% Rh/Pt–30% Rh thermocouple welded to the heater.

Thermal expansion data between room temperature and 1300° C were obtained with a high-temperature dilatometer, using Al_2O_3 as the reference material.

3. Results and discussion

Studies of the phase equilibria were carried out at temperatures ranging from 1150 to ~2000° C. The results of the X-ray analysis are given in Table I.

The results of the high-temperature X-ray diffraction and the thermal expansion studies are summarized in Fig. 1. Some typical thermal expansion curves of zirconia–dysprosia specimens are shown in Fig. 2. Since the temperature of the zirconia inversion on cooling is better difined than that on heating, it was taken as representative. The variation of the temperature of the ZrO_2 transformation with Dy_2O_3 content on cooling is shown in Fig. 3. These data show that the tetragonal–monoclinic transformation temperature (990° C for ZrO_2) decreases steadily with addition of Dy_2O_3 up to 4 mol % Dy_2O_3 and then remains

TABLE I Results of measurements on ZrO_2–Dy_2O_3 compositions

Compositions (mol % Dy_2O_3	Quenching temperature (°C)			
	1150	1450	1765	> 2000
0	Monoclinic ZrO_2			
2	Monoclinic solid solution of ZrO_2 (M_{ss}) + cubic s.s. of fluorite type (F_{ss})			
4	$M_{ss} + F_{ss}$			
6	$M_{ss} + F_{ss}$	$M_{ss} + F_{ss}$	$M_{ss} + F_{ss}$	F_{ss}
8	$M_{ss} + F_{ss}$	$M_{ss} + F_{ss}$	F_{ss}	F_{ss}
9	F_{ss}	F_{ss}	F_{ss}	F_{ss}
10	F_{ss}	F_{ss}	F_{ss}	F_{ss}
15	F_{ss}	F_{ss}	F_{ss}	F_{ss}
20	F_{ss}	F_{ss}	F_{ss}	F_{ss}
30	F_{ss}	F_{ss}	F_{ss}	F_{ss}
35	F_{ss}	F_{ss}	F_{ss}	F_{ss}
40	F_{ss}	F_{ss}	F_{ss}	F_{ss}
45	F_{ss}	F_{ss}	F_{ss}	F_{ss}
50	F_{ss} + hexagonal H_2	F_{ss}	F_{ss}	F_{ss}
55	Hexagonal compound $M_7O_{11.5}$-type (H_2)		$F_{ss} + C_{ss}$	F_{ss}
57	H_2 + hexagonal $H_{3\,ss}$	$H_2 + H_{3ss}$	$F_{ss} + C_{ss}$	$F_{ss} + C_{ss}$
60	$H_2 + H_{3ss}$	$H_2 + H_{3ss}$	$F_{ss} + C_{ss}$	$F_{ss} + C_{ss}$
65	$H_2 + H_{3ss}$	$H_2 + H_{3ss}$	$F_{ss} + C_{ss}$	$F_{ss} + C_{ss}$
70	Hexagonal H_{3ss}	H_{3ss}	C_{ss}	$F_{ss} + C_{ss}$
75	Hexagonal compound M_7O_{11}-type (H_3)		C_{ss}	$F_{ss} + C_{ss}$
80	H_{3ss}	H_{3ss}	C_{ss}	$F_{ss} + C_{ss}$
85	H_{3ss}	H_{3ss}	C_{ss}	C_{ss}
90	H_{3ss}	H_{3ss}	C_{ss}	C_{ss}
95	C_{ss}	C_{ss}	C_{ss}	C_{ss}
100	Cubic dysprosia			Monoclinic B

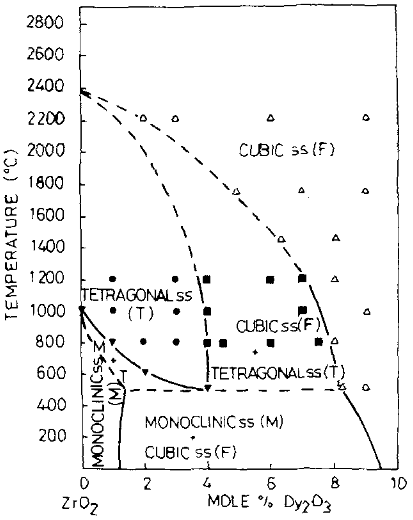

Figure 1 Zirconia-rich region of the tentative zirconia–dysprosia system. Filled circles and squares show results obtained by high-temperature X-ray diffraction; open triangles those found on quenched samples at room temperature; and filled triangles those obtained by dilatometric measurements.

constant. This result indicates that, at temperatures above the tetragonal monoclinic phase transformation of the pure ZrO_2, the tetragonal ZrO_2 solid solution field extends from 0 to 4 mol % Dy_2O_3. Taking into account this feature, the boundary of the tetragonal solid solution is shown at 4 mol % Dy_2O_3 at 500° C. The invariant transformation temperatures for 4 and 6 mol % Dy_2O_3 in the thermal expansion data (Fig. 3) and the varying amounts of co-existing phase with temperature (from the high-temperature X-ray diffraction data) support the contention that a eutectoid transformation (tetragonal ZrO_2 solid solution $\rightarrow$ monoclinic ZrO_2 solid solution + cubic ZrO_2 solid solution) occurs in this vicinity. Our results are in good agreement with the decrease in the transformation temperature also recorded by the dilatometric method by Fehrembacher *et al.* [3], who found that on cooling a composition ZrO_2 – 5 mol % Dy_2O_3 the transformation temperature was 500° C. A similar eutectoid reaction was confirmed by Srivastana *et al.* [4] in the system

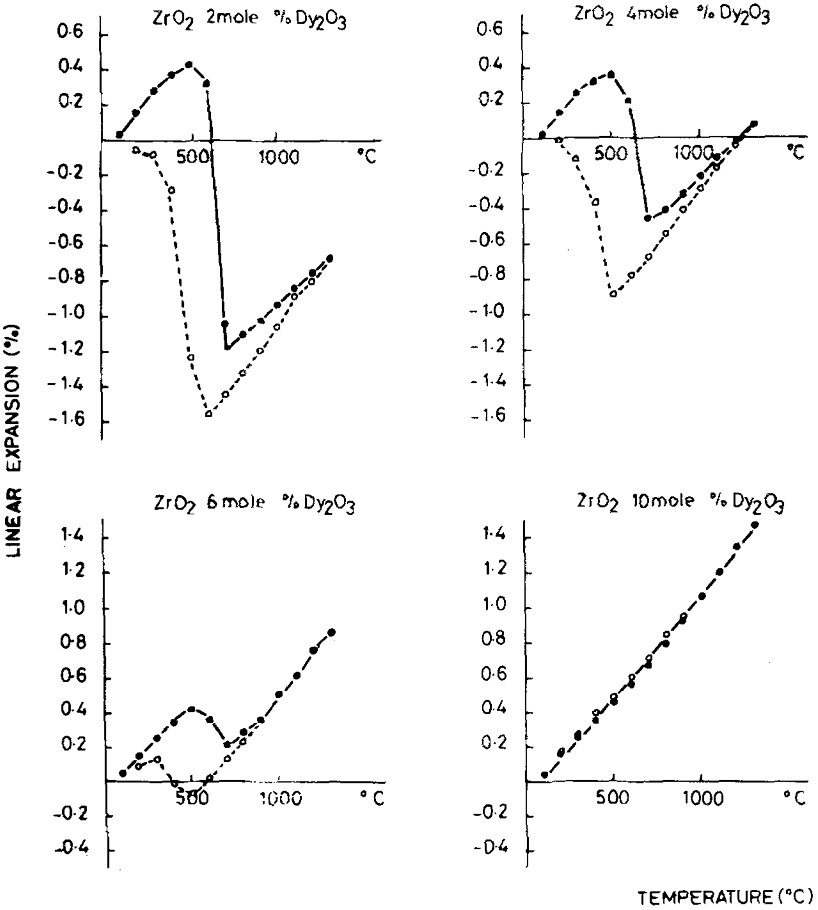

Figure 2 Linear thermal expansion curves for zirconia–dysprosia compositions.

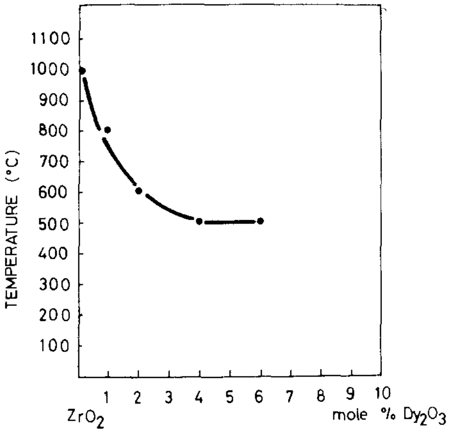

Figure 3 Effect of dysprosia on tetragonal–monoclinic transformation temperature of zirconia on cooling.

ZrO_2–Y_2O_3 and by Duran [5] in the system ZrO_2–Er_2O_3.

At room temperature the solubility of Dy_2O_3 in monoclinic ZrO_2 is ~ 1.5 mol %. Samples with more dysprosia were two-phase, one monoclinic ZrO_2 solid solution and the other cubic ZrO_2 solid solution. This mixture was present between 1.5 and ~ 9.5 mol % Dy_2O_3. Beyond 9.5 mol % Dy_2O_3, a single-phase of fluorite structure is present, the left-hand boundary of the fluorite domain is easily detected by the disappearance of the (1 1 1) and (1 1 $\bar{1}$) monoclinic ZrO_2 solid solution peaks. By determining the lattice parameters of the fluorite phase the lower limit was found to be ~ 8.5 mol % Dy_2O_3 at 500° C, 7 mol % at 1200° C, 6.3 mol % at 1450° C, 5 mol % at 1765° C and ~ 2 mol % at ~ 2000° C (Fig. 1). The boundary is extended to 2370° C to include cubic zirconia [6].

Samples containing >10 mol % Dy_2O_3 which had been melted in a solar furnace and cooled rapidly in water gave a single phase of fluorite structure or C-type. They constitute evidence for a continuous transition between the two at high temperatures, in agreement with the results of Perez y Jorba [1] and Rouanet [2]. However, when these samples were annealed at ~ 1800° C, segregation into two phases occured, and it is possible that the single-phase quenched melt is metastable with respect to a diphasic equilibrium. Effectively, several compositions in the range 50 to 70 mol % Dy_2O_3 which were heat treated above 2000° C showed separation into fluorite and C-type phases, but the parameters of these phases varied with overall sample composition, which indicates clearly that equilibrium was not retained on quenching. This may indicate small composition changes or sample inhomogeneity arising from preferential evaporation so that the results at very high temperatures should be treated with care.

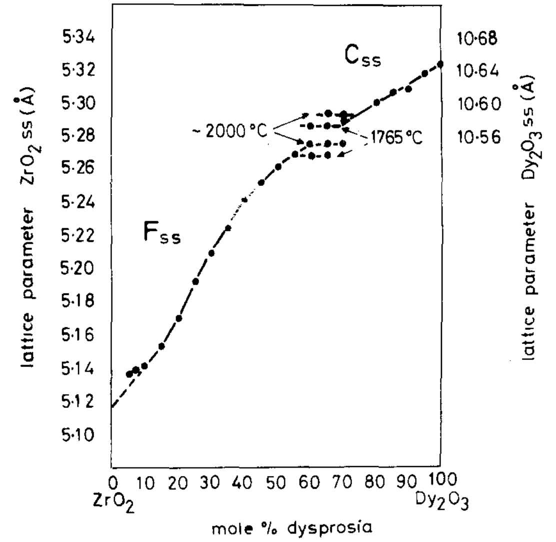

Figure 4 Room-temperature lattice parameters of zirconia–dysprosia compositions quenched from 1765 and 2000° C.

At ~ 2000° C the samples containing < 50 mol % Dy_2O_3 were single phase with a cubic structure. The solid solution is of the fluorite-type and constitutes the so-called stabilized zirconia. These solid solutions are oxygen-deficient with respect to the fluorite composition MO_2 and this discrepancy is accommodated by the presence of vacant sites in the oxygen sublattice.

Between 50 and ~ 70 mol % Dy_2O_3, the samples quenched from 2000° C had two phases, one cubic with the fluorite structure and the other cubic with the C-type structure. This miscibility gap is well established, since when the two-phase field was entered, the composition of the fluorite phase remained constant, and the lattice parameter also remained constant. At the left-hand side, the limits of the two-phase field were defined as 53 mol % Dy_2O_3 at 1765° C and 59% Dy_2O_3 at ~ 2000° C. Fig. 4 shows a plot of lattice parameters versus composition for the system ZrO_2–Dy_2O_3. The results presented here are in good agreement with those reported by Thornber *et al.* [7] for the similar systems based on ZrO_2–Ln_2O_3.

Below 1800° C, one of the goals of the present work was to define the stability and composition

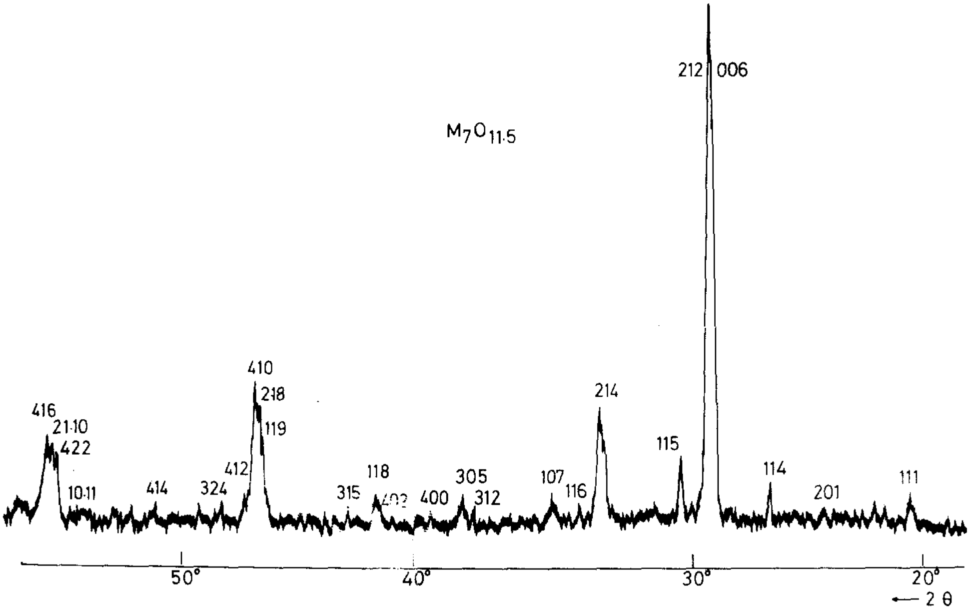

Figure 5 X-ray diffraction pattern of zirconia–dysprosia (55 mol % Dy_2O_3) composition quenched from 1400° C.

of the ordered phases in the system. Sintered and melted samples containing from 30 to 50 mol % Dy_2O_3 were subjected to long-term anneals in the temperature range 800 to 1800° C. After 4 months at 1150° C the only phase present was the fluorite-type solid solution in both kinds of the samples. In the hope of producing the ordered δ-$Dy_4Zr_3O_{12}$ phase, sintered and melted samples containing 40 mol % Dy_2O_3 were annealed up to 6 months between 800 and 1150° C. After this heat treatment, the ordered δ-$Dy_4Zr_3O_{12}$ phase was not seen. This result indicates that if the formation of the ordered δ-phase required ordering of the oxygen sublattice only, then presumably such a phase would have formed. However, taking into account the large size variation between the cation radii of the Dy^{3+} (0.93 Å) and Zr^{4+} (0.79 Å), it is probable that its formation would require complete metal ordering and, if this is so, the low metal diffusion rate is a large diffculty in obtaining complete reaction at low temperatures. Although no evidence was found for the ordered δ-phase by X-ray diffraction, it is possible that by utilizing other techniques, such as electron diffraction or HRTM, the ordered δ-phase can be observed. This study is now in progress.

Compositions containing > 50 mol % Dy_2O_3 show a complex picture of phase transformation in the system. Between 55 and 60 mol % Dy_2O_3 hexagonal phase of the $M_7O_{11.5}$-type was found. This compound is isostructural with the hexagonal phase H_2 previously found by Perez y Jorba [1] in the ZrO_2–Ln_2O_3 (Ln = Gd, Dy and Yb) systems. Fig. 5 shows the X-ray diffraction powder diagram for 55 mol % Dy_2O_3. The lattice parameters measured on compositions at both sides of the ideal $M_7O_{11.5}$ composition remained constant. Therefore, it suggests that the hexagonal compound $M_7O_{11.5}$ (55 mol % Dy_2O_3) may be a line in this system or, at least, has a very narrow homogeneity range. It exists over the temperature range 800 to 1750° C; above this temperature it decomposes into cubic phase of the fluorite and C-types. Some differences exist with respect to the similar ZrO_2–Dy_2O_3 [1]. In this system the hexagonal compound (45 mol % ZrO_2–55 mol % Dy_2O_3) was found to be stable between 1450 and 1700° C; above this temperature it decomposes into a cubic phase of the fluorite-type, and below 1450° C it decomposes into two cubic phases of the C-type. In the present work, no evidence was found for the co-existence of two C-type phases. A composition containing 55 mol % Dy_2O_3, annealed at 1400° C for 500 h was a well-defined hexagonal phase of the $M_7O_{11.5}$-type, and this structure was also present below this temperature. It should be mentioned that occasionaly and under certain conditions (for example, in some melted samples annealed several days at 1150° C) two C-type phases co-existed. This feature, according with the results of Scott [8] on the ZrO_2–Y_2O_3 system, can be explained as a metastable situation which occurs

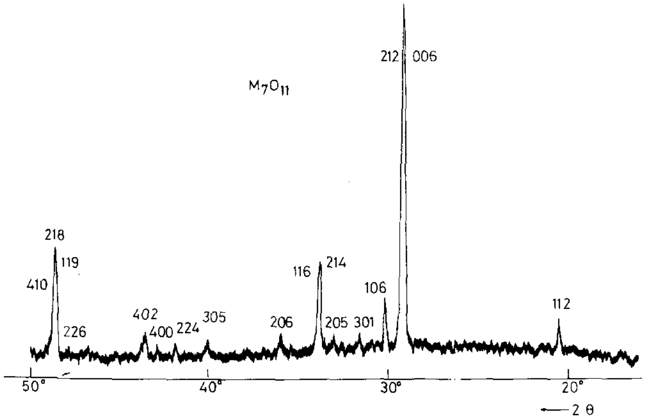

Figure 6 X-ray diffraction pattern of zirconia–dysprosia (70 mol% Dy_2O_3) composition quenched from 1550° C.

in samples initially treated at high temperatures, taking into account the different solubility of zirconia in dysprosia with temperature.

Sintered and melted samples containing 65 to 90 mol % Dy_2O_3 and annealed below 1700° C were another hexagonal phase of the M_7O_{11}-type. This phase is isostructural with the hexagonal compound H_3 previously formed in the ZrO_2–Gd_2O_3, ZrO_2–Dy_2O_3 and ZrO_2–Yb_2O_3 systems [1]. Fig. 6 shows the X-ray diffraction powder diagram for this phase. In agreement with the data of Spiridinov *et al.* [9], this hexagonal phase represents a compound with the composition Dy_6ZrO_{11} (close to the composition 75 mol % Dy_2O_3); its unit cell contains six molecules of compound, i.e. $Dy_{42}O_{66} = 36\ Dy^{3+}, 6Zr^{4+}, 66O^{2-}$, 18□ and its region of homogeneity extends from ~65 to 90 mol % Dy_2O_3 at 1150° C. The phase exists over the temperature range 800 to 1700° C, and above this temperature it is reversibly transformed into a C-type cubic solid solution probably by an order–disorder transition. Table II shows the results obtained in samples annealed for 4 months at 1150° C in the concentration range 50 to 90 mol % Dy_2O_3.

It should be mentioned that in the work of Thornber *et al.* [7], no evidence was found for the existence of these hexagonal phases at high Ln_2O_3 content. However, no detailed studies of the order–disorder transition of these compounds is known. Therefore, until the detailed structure of M_7O_{11}-type compounds is determined, it is not possible to reach definitive conclusions about this.

At > 2000° C the diagram is drawn as simply as possible in accordance with phase rules, so that it will not conflict with the liquidus curve of Rouanet [2] for the system ZrO_2–Dy_2O_3. However, taking into account the decrease in the solubility of zirconia in dysprosia as the temperature increases, the subsolidus boundaries were correlated with the liquidus measurements of Rouanet [2] as a means of incorporating the diphasic domain (fluorite-type + C-type solid solutions) which appears to extend to the solidus (Fig. 7).

4. Conclusions

Phase relationships have been established for this binary system in the 0 to 100 mol % Dy_2O_3 composition range. Additional work will be necassary to determine unequivocally the complete diagram

TABLE II Phases and lattice parameters in samples annealed for 4 months at 1150° C

Composition (mol % Dy_2O_3)	Phases	Parameters (Å)
50	Fluorite solid solution + H_2 (very diffuse)	$a =$ 5.2591
55	H_2	$a =$ 9.8793 $c =$ 18.2277
57	H_2 H_3 (very diffuse)	$a =$ 9.8677 $c =$ 18.2248
60	H_2 H_3	$a =$ 9.8880 $c =$ 18.2257
65	H_2 (very diffuse) H_3 solid solution	$a =$ 9.8822 $c =$ 18.5042
70	H_3 solid solution	$a =$ 9.8909 $c =$ 18.5661
75	H_3	$a =$ 9.9288 $c =$ 18.5838
80	H_3	$a =$ 9.9237 $c =$ 18.6503
90	H_3 (diffuse) C-Type	$a =$ 10.6210

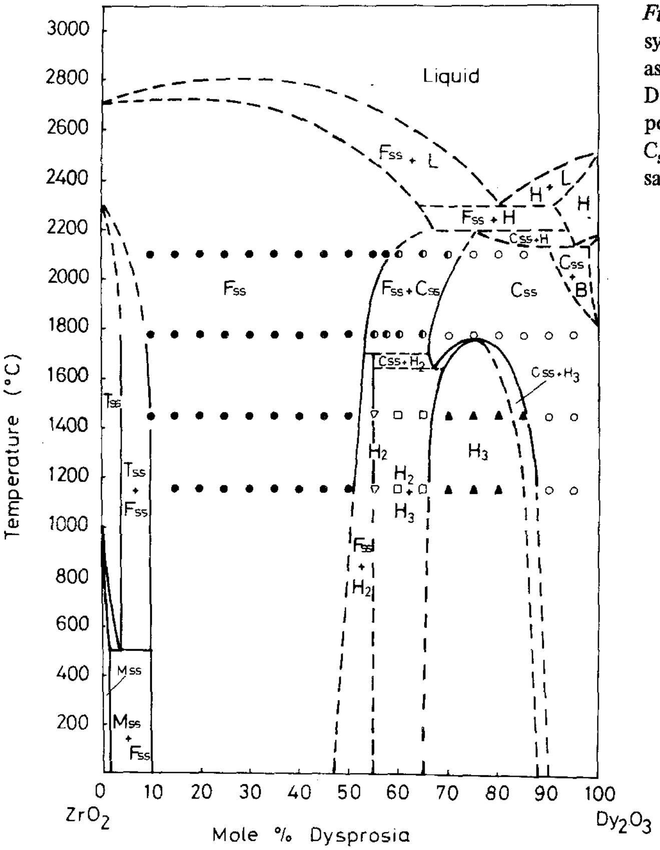

Figure 7 Phase diagram for zirconia–dysprosia system. M_{ss}, T_{ss} and F_{ss} have the same meaning as in Fig. 1; H_2 = hexagonal compound (55mol% Dy_2O_3) (quenched samples); H_2 = hexagonal compound (75mol% Dy_2O_3) (quenched samples). C_{ss} = cubic dysprosia solid solution (quenched samples).

and the exact location of phase boundaries, but the tentative diagram proposed here is in accord with the phase rules and incorporates the following results.

(1) The solubility of Dy_2O_3 in monoclinic ZrO_2 is ~ 1.5 mol % at room temperature. The lower boundary of the tetragonal zirconia solid solution region of the phase diagram was defined taking into account the tetragonal–monoclinic inversion temperature of zirconia. Therefore, the boundary line up to 4 mol % Dy_2O_3 was traced from the dilatometric measurements and high-temperature X-ray diffraction studies (Figs. 1 and 3). The existence of a two-phase region, monoclinic + cubic zirconia solid solution, between ~ 1.5 and ~ 9.5 mol % Dy_2O_3 below 500° C leads to the assumption that there is a eutectoid reaction between monoclinic and cubic zirconia.

(2) An extensive cubic solid solution region extends from ~ 9.5 to 47 mol % Dy_2O_3 at room temperature and from ~ 2 to 59 mol % Dy_2O_3 at ~ 2000° C. By using the precision lattice parameter method (Fig. 4) the width of this field was determined at 1150, 1450, 1765 and ~ 2000° C.

(3) There is also a two-phase region of fluorite and C-type solid solutions from 53 to 67 mol % Dy_2O_3 at 1765° C and from 59 to 73 mol % Dy_2O_3 at ~ 2000° C. Within this area two hexagonal compounds were present in the system at low temperatures (< 1765° C): one of the $M_7O_{11.5}$-type (55 mol % Dy_2O_3) and the other of the M_7O_{11}-type (75 mol % Dy_2O_3).

(4) At high Dy_2O_3 content (> 65 mol %) there is a single-phase of the C-type solid solution above 1765° C. This region becomes somewhat broader at room temperature.

(5) The tentative phase diagram of the system ZrO_2–Dy_2O_3 (Fig. 7) utilizes the data of Rouanet [2] for the liquidus and for the region containing fluorite solid solution (F_{ss}) and hexagonal Dy_2O_3 (H_{ss}).

Acknowledgement

The author thanks Dr J. P. Coutures of the Laboratoire des Ultrarrefractaires, Odeillo, France, for the facilities given for sample preparation in the solar furnace.

References

1. M. PEREZ Y JORBA, *Ann. Chim.* 7 (1962) 479.
2. A. ROUANET, *Compt. Rend. Acad. Sci. Paris* 267c (1968) 1581.
3. L. L. FEHRENBACHER, L. A. JACOBSON and C. T. LYNCH, in "Proceeding of Four Rare Earth Conference", edited by L. Eyring, (Gordon and Breach, New York, 1965) p. 687.
4. K. K. SRIVASTAVA, R. N. PATIL, C. B. CHOUDHARY, K. V. G. K. GOKHALE and E. C. SUBBARAO, *Trans. J. Brit. Ceram. Soc.* 73 (1974) 85.
5. P. DURAN, *J. Amer. Ceram. Soc.* 60 (1977) 510.
6. G. M. VOLTEN, *ibid* 46 (1963) 418.
7. M. R. THORNBER, D. J. M. BEVAN and E. SUMMERVILLE, *J. Solid State Chem.* 1 (1970) 545.
8. H. G. SCOTT, *J. Mater. Sci.* 12 (1977) 311.
9. F. M. SPIRIDINOV, V. A. STEPANOV, L. N. KOMISSAROVA and V. I. SPITSYN, *J. Less Common Met.* 14 (1968) 435.

Received 9 October and accepted 20 November 1979.